Electronic Supplementary Information

$Sb_4O_5Cl_2$ Embedded in Carbon Polyhedra For Fast Charge Kinetics Towards High-Capacity Lithium-ion Capacitors

Meng Wang,[ab] Kewei Liu,[ac] Yanan Xu,[ac] Xudong Zhang,[ac] Qifan Peng,[a] Yang Guo,[a] Xiong Zhang,[ac] Xianzhong Sun,[ac] Weiwei Pang,*[e] Kai Wang,*[ac] Le Yu,*[b] Yanwei Ma*[acd]

[a]*Institute of Electrical Engineering, Chinese Academy of Sciences*

Beijing 100190, P. R. China

E-mail: wangkai@mail.iee.ac.cn; ywma@mail.iee.ac.cn

[b]*State Key Lab of Organic-Inorganic Composites, Beijing University of Chemical Technology, Beijing, 100029, P. R. China*

E-mail: yule@mail.buct.edu.cn

[c]*School of Engineering Sciences, University of Chinese Academy of Sciences*

Beijing 100049, P. R. China

[d]*School of Materials Science and Engineering, Zhengzhou University*

Zhengzhou 450001, P. R. China

[e]*Petrochemical Research Institute, PetroChina Company Limited, Beijing 102206, P. R. China*

E-mail: pangweiwei@petrochina.com.cn

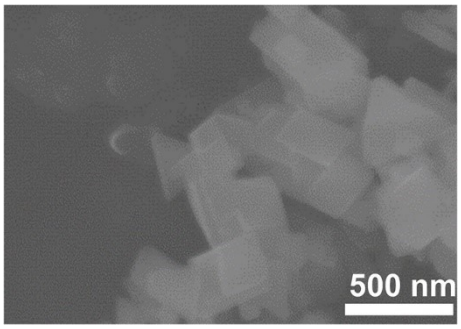

Fig. S1 Field-emission scanning electron microscopy (FESEM) image of $Sb_4O_5Cl_2$.

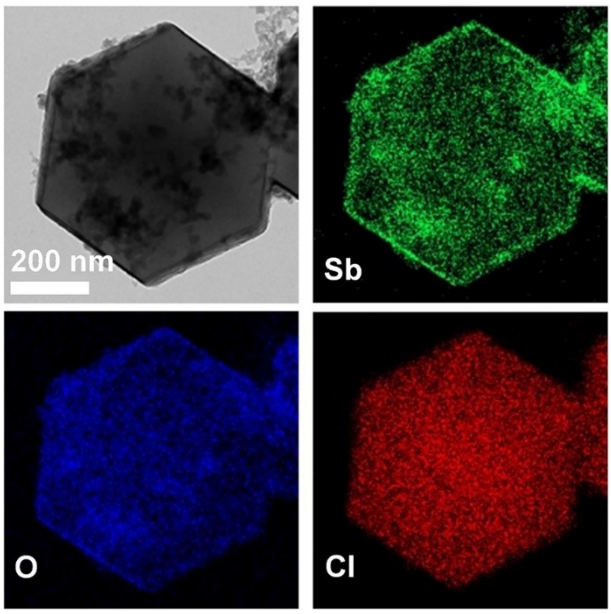

Fig. S2 Transmission electron microscopy and the corresponding elemental mapping images of $Sb_4O_5Cl_2$@ZCP.

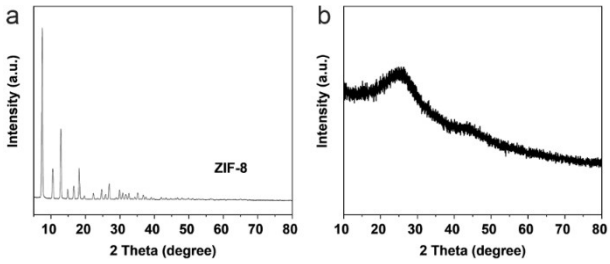

Fig. S3 X-ray diffraction (XRD) patterns of (a) ZIF-8 and (b) ZCP.

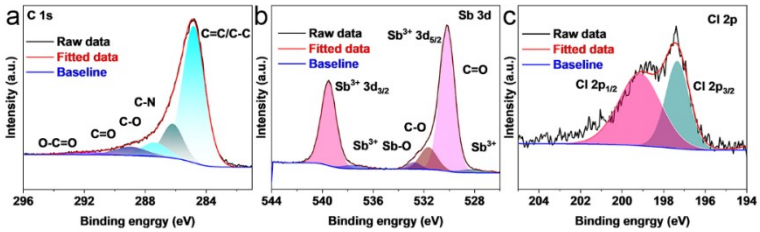

Fig. S4 (a) C 1s XPS spectrum, (b) Sb 3d XPS spectrum, and (c) Cl 2p XPS spectrum of $Sb_4O_5Cl_2$@ZCP.

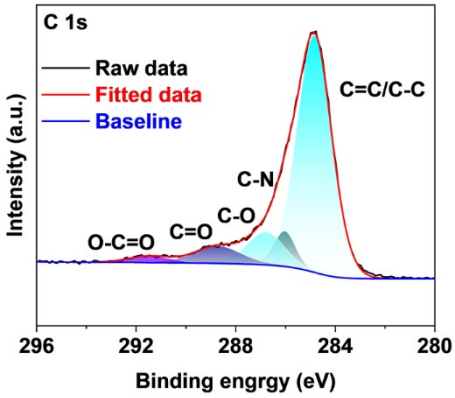

Fig. S5 C 1s XPS spectrum of ZCP.

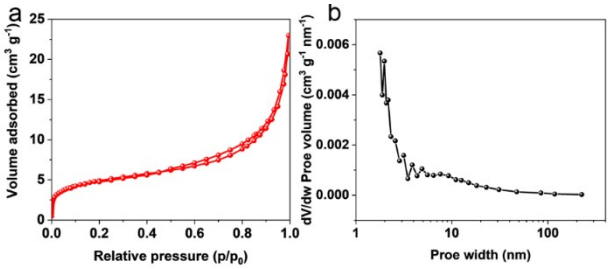

Fig. S6 (a) N_2 adsorption-desorption isotherms, and (b) pore size distribution curve of $Sb_4O_5Cl_2$@ZCP.

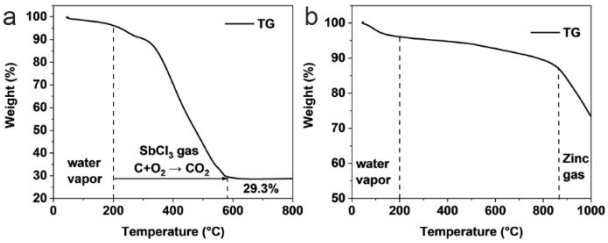

Fig. S7 Thermogravimetry curves of (a) $Sb_4O_5Cl_2$@ZCP in air and (b) ZCP in N_2.

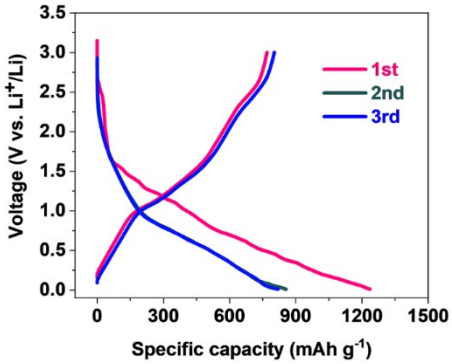

Fig. S8 Galvanostatic charge-discharge (GCD) profiles of the initial 3 cycles at 0.1 A g^{-1} for $Sb_4O_5Cl_2$@ZCP.

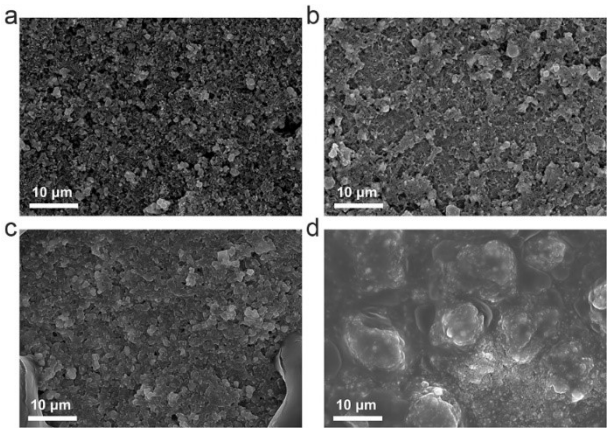

Fig. S9 FESEM images of (a,c) $Sb_4O_5Cl_2$ and (b,d) $Sb_4O_5Cl_2$@ZCP anodes (a,b) before and (c,d) after cycling.

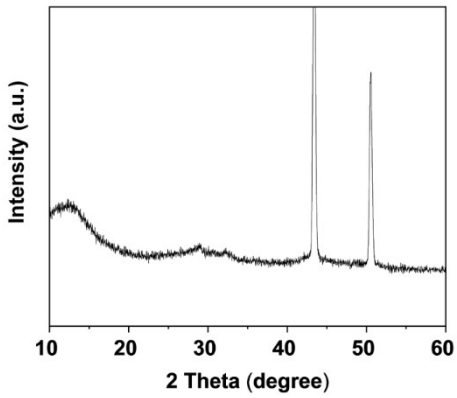

Fig. S10 XRD pattern of $Sb_4O_5Cl_2$@ZCP after cycling.

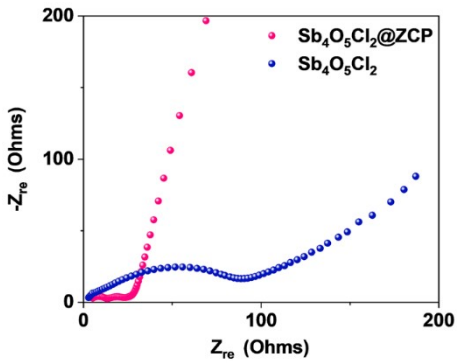

Fig. S11 Nyquist plots of $Sb_4O_5Cl_2$@ZCP and $Sb_4O_5Cl_2$ electrodes.

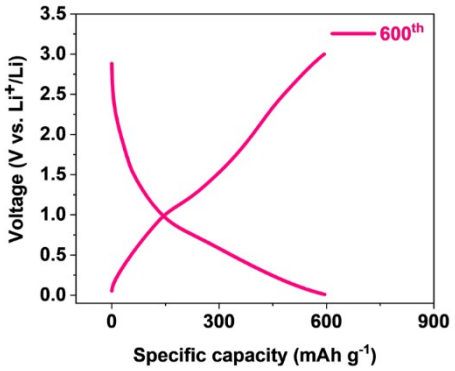

Fig. S12 GCD profiles of the $Sb_4O_5Cl_2$@ZCP after long-term cycling.

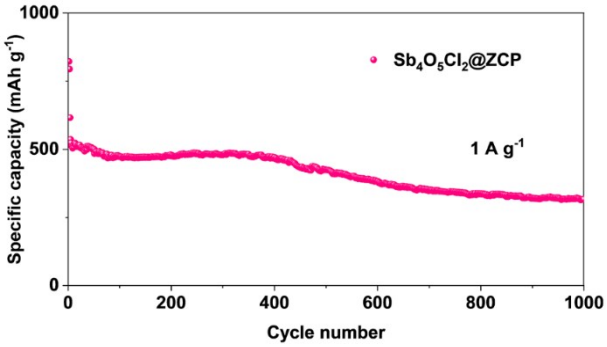

Fig. S13 Cycling performance of $Sb_4O_5Cl_2$@ZCP.

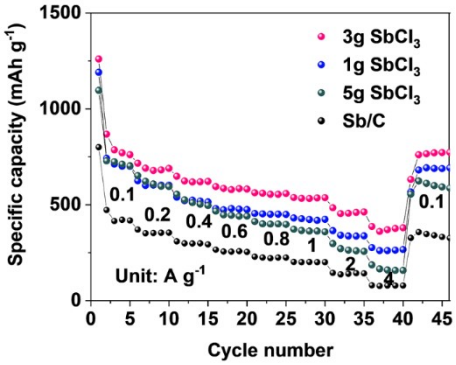

Fig. S14 Rate performance of Sb/C and $Sb_4O_5Cl_2$@ZCPs using different amounts of $SbCl_3$.

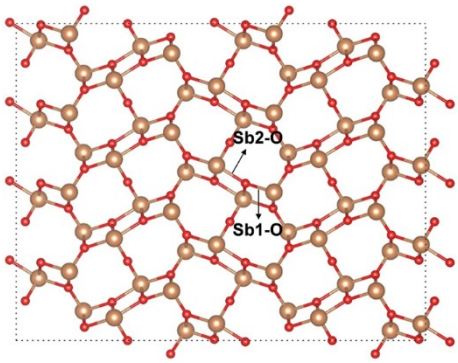

Fig. S15 Sb1-O and Sb2-O coordination bonds in $Sb_4O_5Cl_2$.

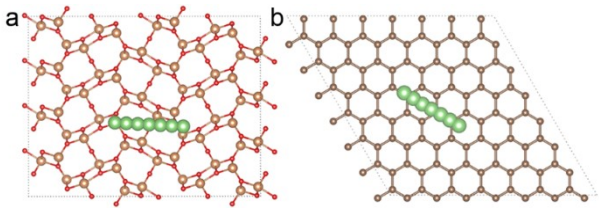

Fig. S16 Li^+ migration paths in the surfaces of (a) $Sb_4O_5Cl_2$ and (b) ZCP.

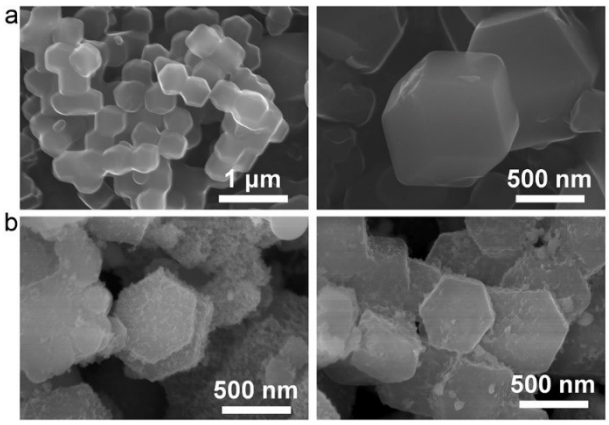

Fig. S17 FESEM images of (a) $Sb_3O_2F_5$@ZCP and (b) SbOBr@ZCP.

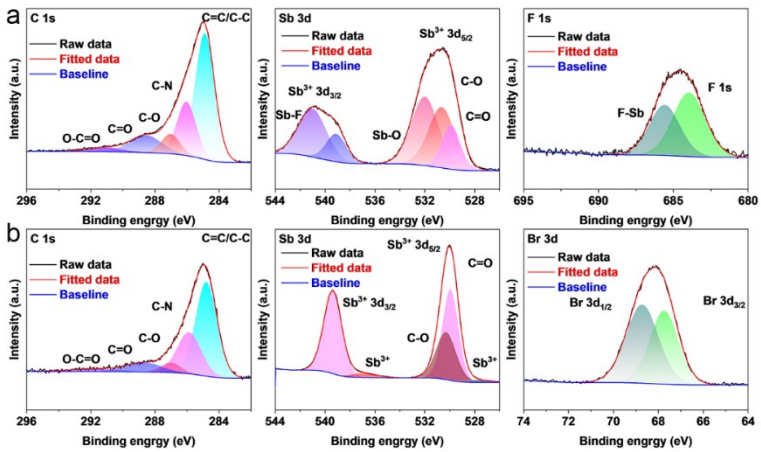

Fig. S18 XPS spectra of (a) $Sb_3O_2F_5$@ZCP and (b) SbOBr@ZCP.

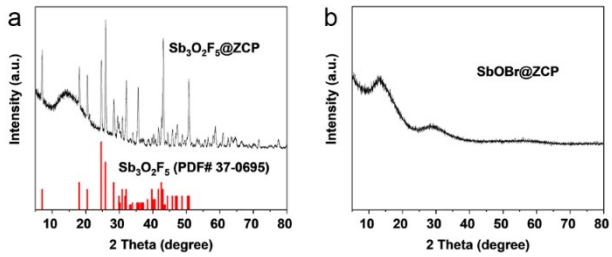

Fig. S19 XRD patterns of (a) $Sb_3O_2F_5$@ZCP, and (b) SbOBr@ZCP.

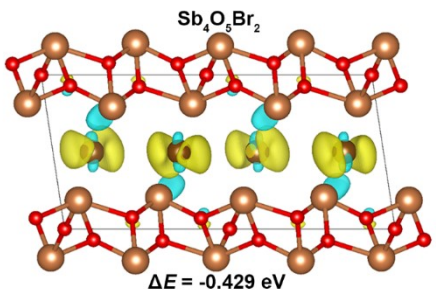

Fig. S20 Electron density differences of $Sb_4O_5Br_2$.

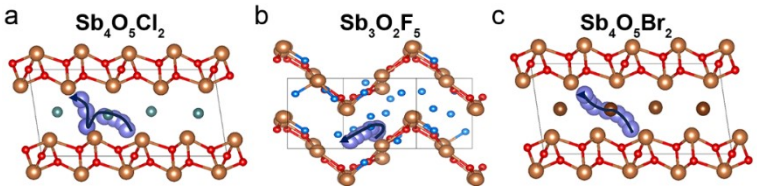

Fig. S21 Li^+ migration paths in the interlayers of (a) $Sb_4O_5Cl_2$, (b) $Sb_3O_2F_5$ and (c) $Sb_4O_5Br_2$.

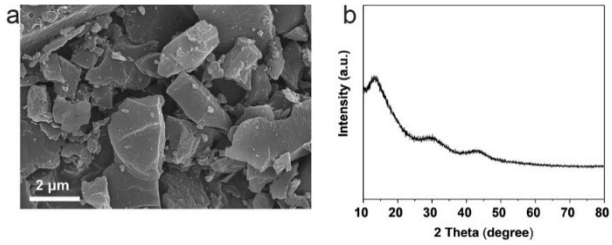

Fig. S22 FESEM image and XRD pattern of YP-80F.

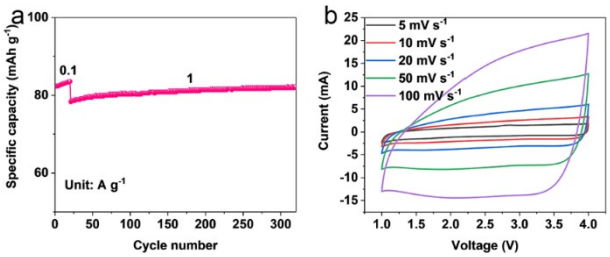

Fig. S23 (a) Cycling performance and (b) CV curves of YP-80F cathode.

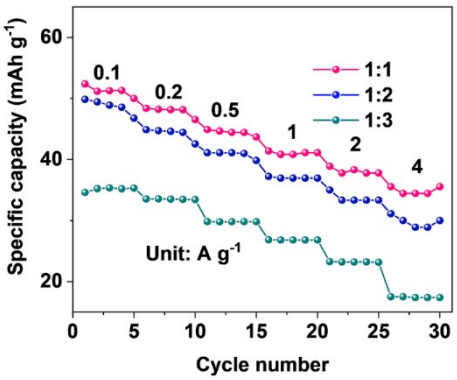

Fig. S24 Rate performance of different mass ratios of cathode and anode in a LIC device.

Table S1 Elemental contents in ZCP and $Sb_4O_5Cl_2$@ZCP determined by XPS.

Sample	Atomic concentration (at.%)			
	C	**O**	**Zn**	**Sb**
ZCP	79.43	15.97	4.59	/
$Sb_4O_5Cl_2$@ZCP	40.51	49.5	2.8	7.19

Table S2 ICP results of $Sb_4O_5Cl_2$@ZCP sample.

Sample	Sb (wt%)	Zn (wt%)
$Sb_4O_5Cl_2$@ZCP	9.4	3.65

Table S3 Comparison table of $Sb_4O_5Cl_2$@ZCP with other Sb-based anodes.

Anode	Performance	Ref.
$Sb_4O_5Cl_2$@ZCP	601.1 mAh g^{-1} at 0.5 A g^{-1} after 600 cycles	This work
$BiSbSe_3$	428 mAh g^{-1} at 0.1 A g^{-1} after 100 cycles	1
Sb@$Ni_3(HHTP)_2$-10	590 mAh g^{-1} at 0.1 A g^{-1} after 100 cycles	2
Sb nanoflakes	300 mAh g^{-1} at 0.5 A g^{-1} after 80 cycles	3
SS/H@C	624.5 mAh g^{-1} at 10 A g^{-1} after 100 cycles	4
YS-SbC	584 mAh g^{-1} at 0.2 A g^{-1} after 100 cycles	5
$Sb_{30}P_{30}$	807 mAh g^{-1} at 5 A g^{-1} after 200 cycles	6
SnSb@CNF/CFT	208 mAh g^{-1} at 0.5 A g^{-1} after 700 cycles	7
Sb@B_MX_HF5 (6:4)	434 mAh g^{-1} at 0.1 A g^{-1} after 100 cycles	8
NC@SnSb@NC	598 mAh g^{-1} at 0.5 A g^{-1} after 100 cycles	9
SZS-Sisal	638 mAh g^{-1} at 0.5 A g^{-1} after 100 cycles	10
Sb_2S_3@C	450 mAh g^{-1} at 0.5 A g^{-1} after 70 cycles	11
Co-Sb-S@NC	884.9 mAh g^{-1} at 1 A g^{-1} after 400 cycles	12

Supplementary References

1. W.-C. Lin, Y.-C. Yang and H.-Y. Tuan, *Energy Storage Mater.*, 2022, **51**, 38-53.
2. A. Nazir, H. T. T. Le, A.-G. Nguyen, J. Kim and C.-J. Park, *Chem. Eng. J.*, 2022, **450**, 138408.
3. R. Shao, Z. Sun, L. Wang, J. Pan, L. Yi, Y. Zhang, J. Han, Z. Yao, J. Li, Z. Wen, S. Chen, S. Chou, D.-L. Peng and Q. Zhang, *Angew. Chem., Int. Ed.*, 2024, **63**, e202320183.
4. W. Zhao, S. Yuan, S. Lei, Z. Zeng, J. Dong, F. Jiang, Y. Yang, W. Sun, X. Ji and P. Ge, *Adv. Funct. Mater.*, 2022, **33**, 2211542.
5. X. Yang, Y. Zhu, D. Wu, M. Li, Y. He, L. Huang and M. Gu, *Adv. Funct. Mater.*, 2022, **32**, 2111391.
6. Y. Wei, J. He, J. Zhang, M. Ou, Y. Guo, J. Chen, C. Zeng, J. Xu, J. Han, T. Zhai and H. Li, *Energy Environ. Mater.*, 2022, **6**, e12336.
7. Z. Song, G. Wang, Y. Chen, Y. Lu and Z. Wen, *Chem. Eng. J.*, 2023, **463**, 142289.
8. S. Arnold, A. Gentile, Y. Li, Q. Wang, S. Marchionna, R. Ruffo and V. Presser, *J. Mater. Chem. A*, 2022, **10**, 10569-10585.
9. X. Shi, W. Liu, D. Zhang, C. Wang, J. Zhao, X. Wang, B. Chen, L. Chang, Y. Cheng and L. Wang, *Chem. Eng. J.*, 2022, **431**, 134318.
10. H. Qin, B. Zhang, C. Wang, D. Wang and X. Ou, *Energy Storage Mater.*, 2022, **52**, 189-200.
11. H. Ye, Z. Wang, J. Yan, Z. Wang, J. Chen, Q. Dai, Y. Su, B. Guo, H. Li, L. Geng, C. Du, J. Wang, Y. Tang, L. Zhang, L. Zhu and J. Huang, *Adv. Funct. Mater.*, 2022, **32**, 2204231.
12. T. Yan, F. Wen, J. Duan, C. Zhu, J. Wen, Y. Wang, J. Tong and Z. Chen, *Chem. Eng. J.*, 2023, **474**, 145839.